

Tuning of plasmonic surface lattice resonances: on the crucial impact of the excitation efficiency of grazing diffraction orders

Lynda Dehbi,[†] Kartikey Pandey,[‡] Macilia Braïk,[†] Stéphanie Lau-Truong,[‡] Abderrahmane Belkhir,[†]
Sarra Gam-Derouich,[‡] Alexandre Chevillot-Biraud,[‡] Claire Mangeney,[¶] Abdelaziz Mezeghrane,[†] Fadi
Issam Baida,[§] and Nordin Félidj^{*,‡}

[†]*Université Mouloud Mammeri de Tizi Ouzou, LPCQ, BP 17 RP, 15000 Tizi-Ouzou, Algeria*

[‡]*Université Paris Cité, ITODYS, CNRS, F-75006 Paris, France*

[¶]*Université Paris Cité, CNRS, Laboratoire de Chimie et de Biochimie Pharmacologiques et
Toxicologiques, F-75006 Paris, France*

[§]*Université de Bourgogne Franche-Comté, FEMTO-ST, CNRS, 25030 Besançon Cedex, France*

E-mail: nordin.felidj@u-paris.fr

Supporting information

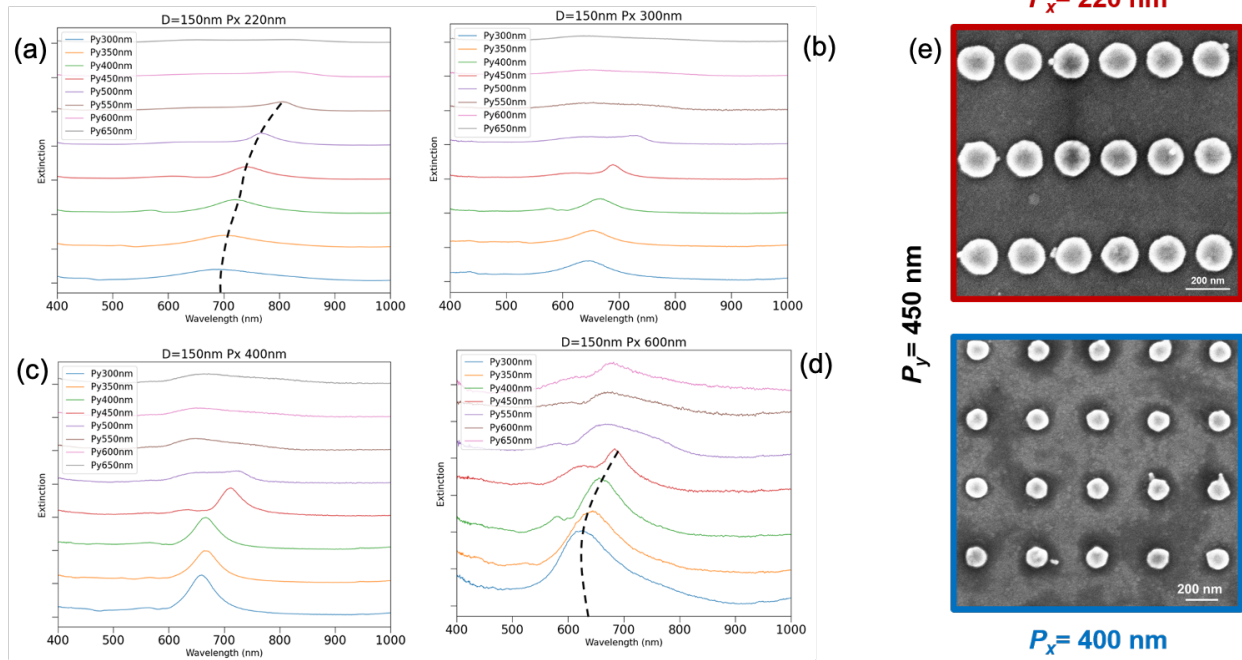


Figure SI 1: Experimental extinction spectra of rectangular array of gold disk of $D=150\text{nm}$ and period $P_x =$ (a) 220nm, (b) 300nm, (c) 400nm and (d) 600nm, the black dotted line in (a) and (d) depict the shift of resonance response with change in P_y

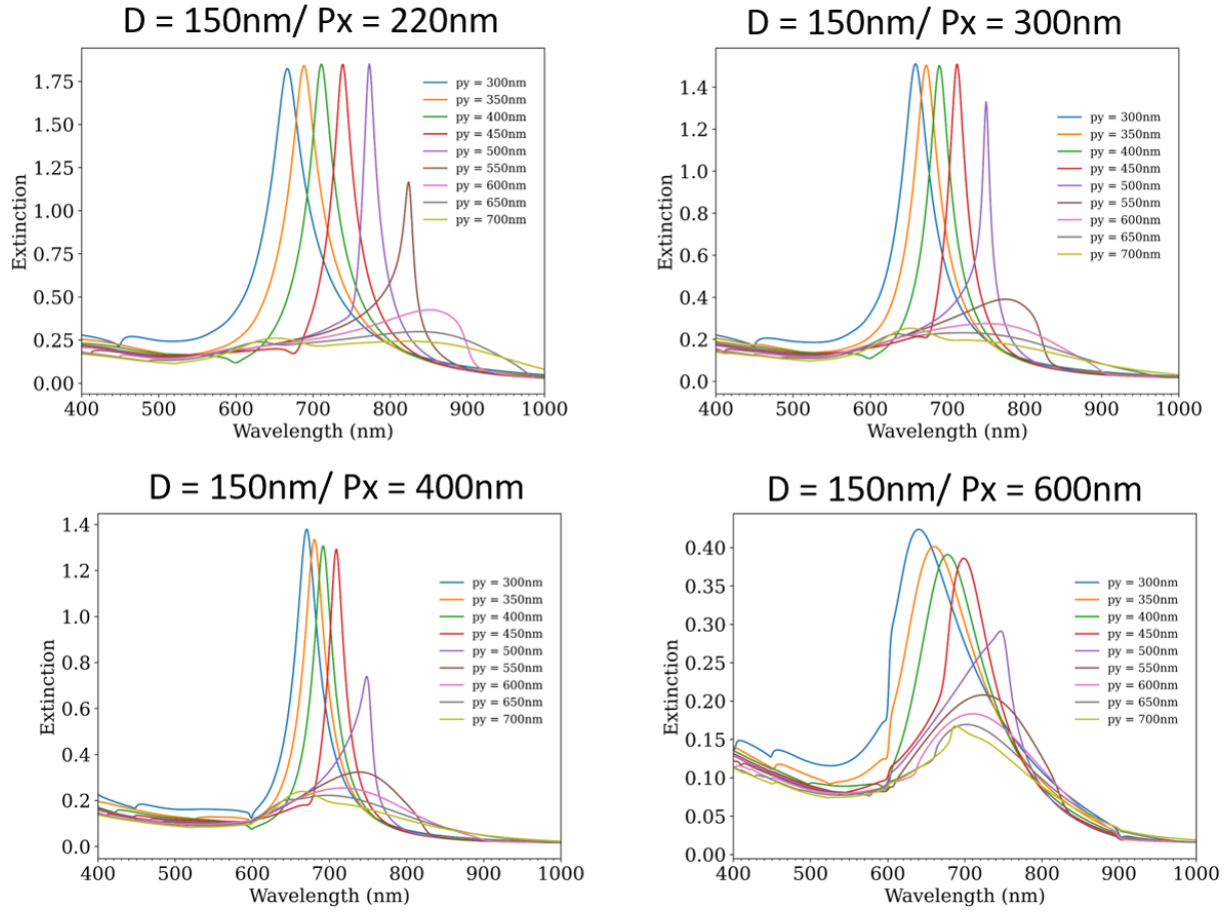


Figure SI 2: ((a-d) calculated extinction spectra of the rectangular arrays of gold disks of diameter $D=150\text{nm}$ and height $h=50\text{nm}$ deposited on a glass substrate coated by a thin ITO layer for fixed $P_x = 220\text{nm}$, 300nm , 400nm and 600nm , in this order. The polarization direction is along the X axis.

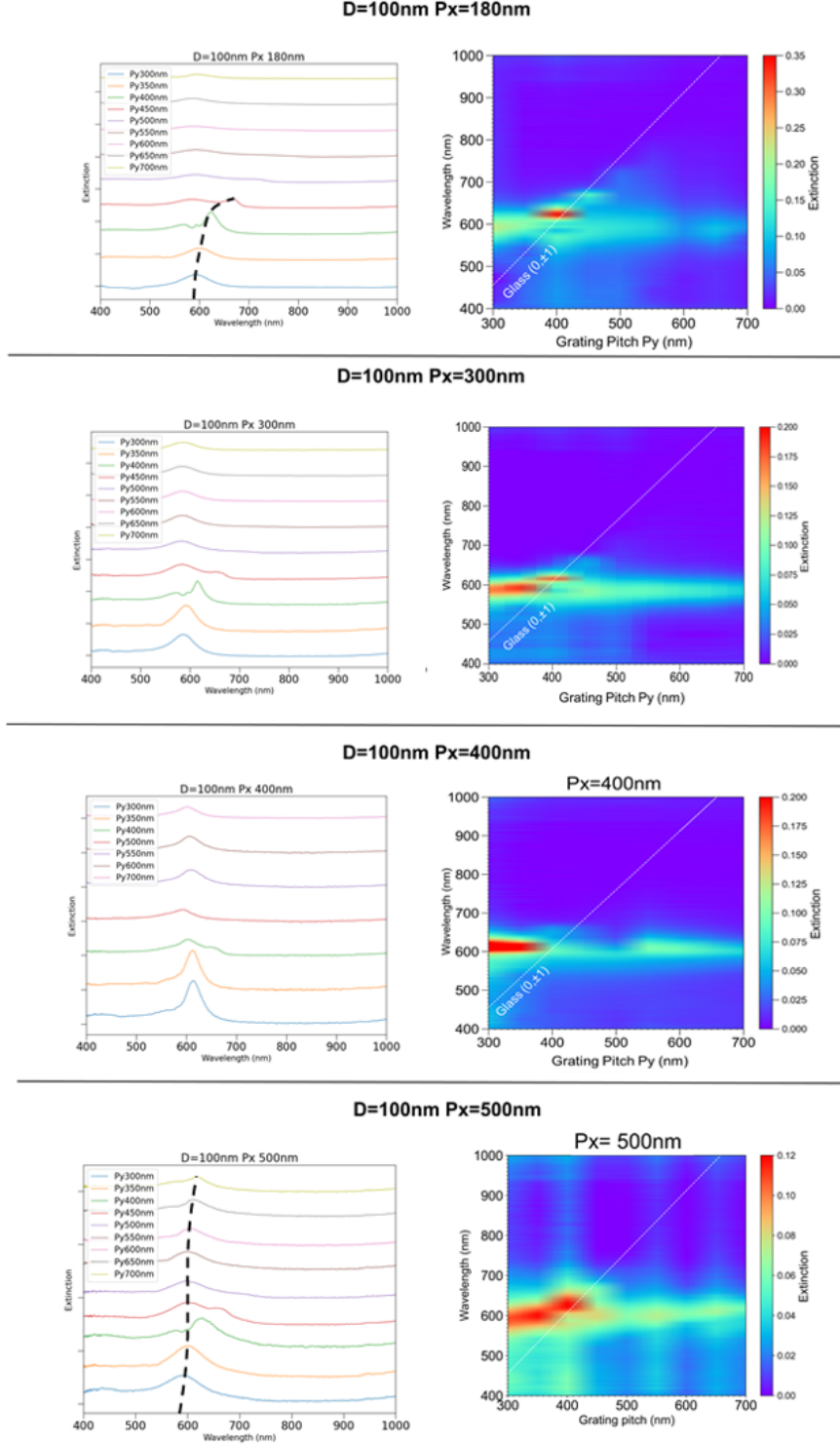


Figure SI 3: (a-d) Experimental Extinction and dispersion diagrams of the rectangular arrays of $D=100\text{nm}$ for fixed $P_X =$ (a) 160nm , (b) 180nm , (c) 300nm and (d) 400nm , respectively. The polarization direction is along the X axis. For the extinction spectra, the black dotted line in (a) and (d) depict the shift of resonance response with change in P_y . Meanwhile for the dispersion diagram, the Rayleigh anomaly position is displayed in a white line for the $(0, \pm 1)$ orders in the substrate.

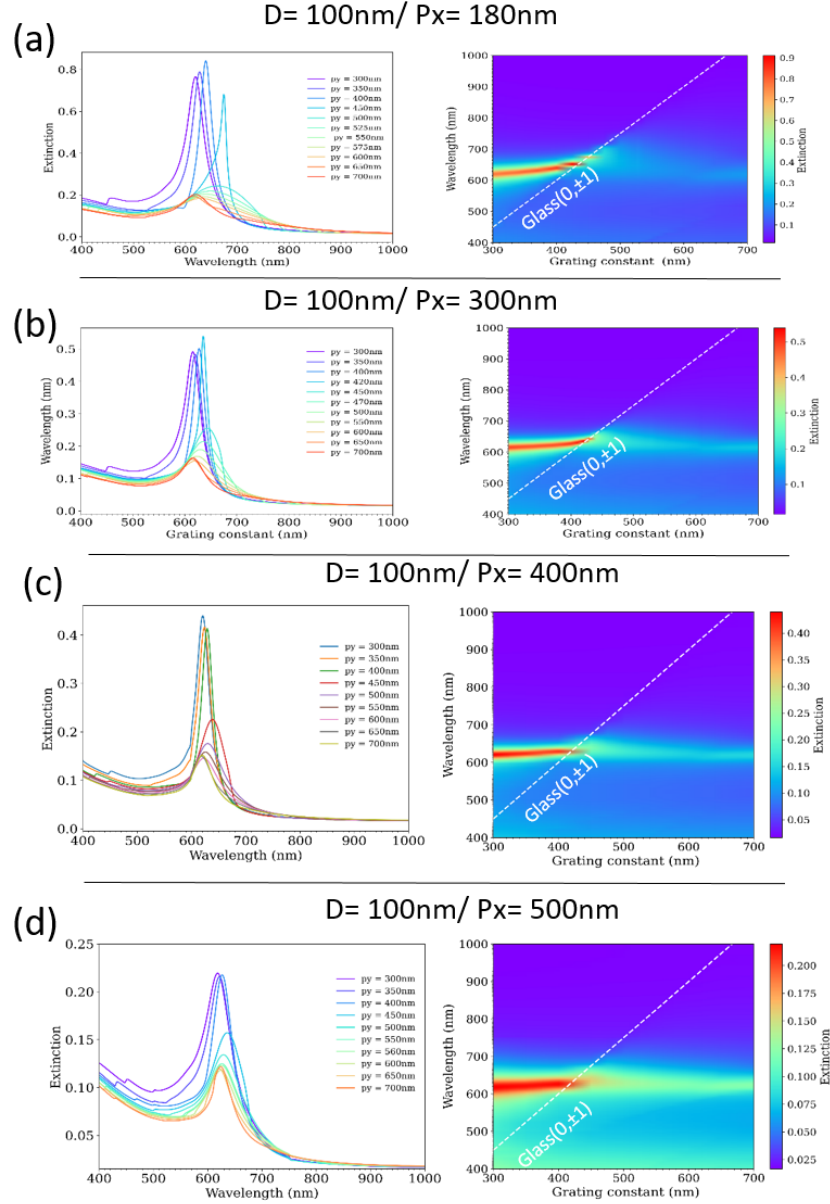


Figure SI 4: (a-d) Calculated extinction and dispersion diagrams of the rectangular arrays of $D = 100\text{nm}$ for fixed $P_x =$ (a)180nm,(b)300nm,(c)400nm and (d)500nm ,respectively. The polarization direction is along the X axis. For the dispersion diagram, the Rayleigh anomaly position is displayed in a white line for the $(0, \pm 1)$ orders in the substrate.

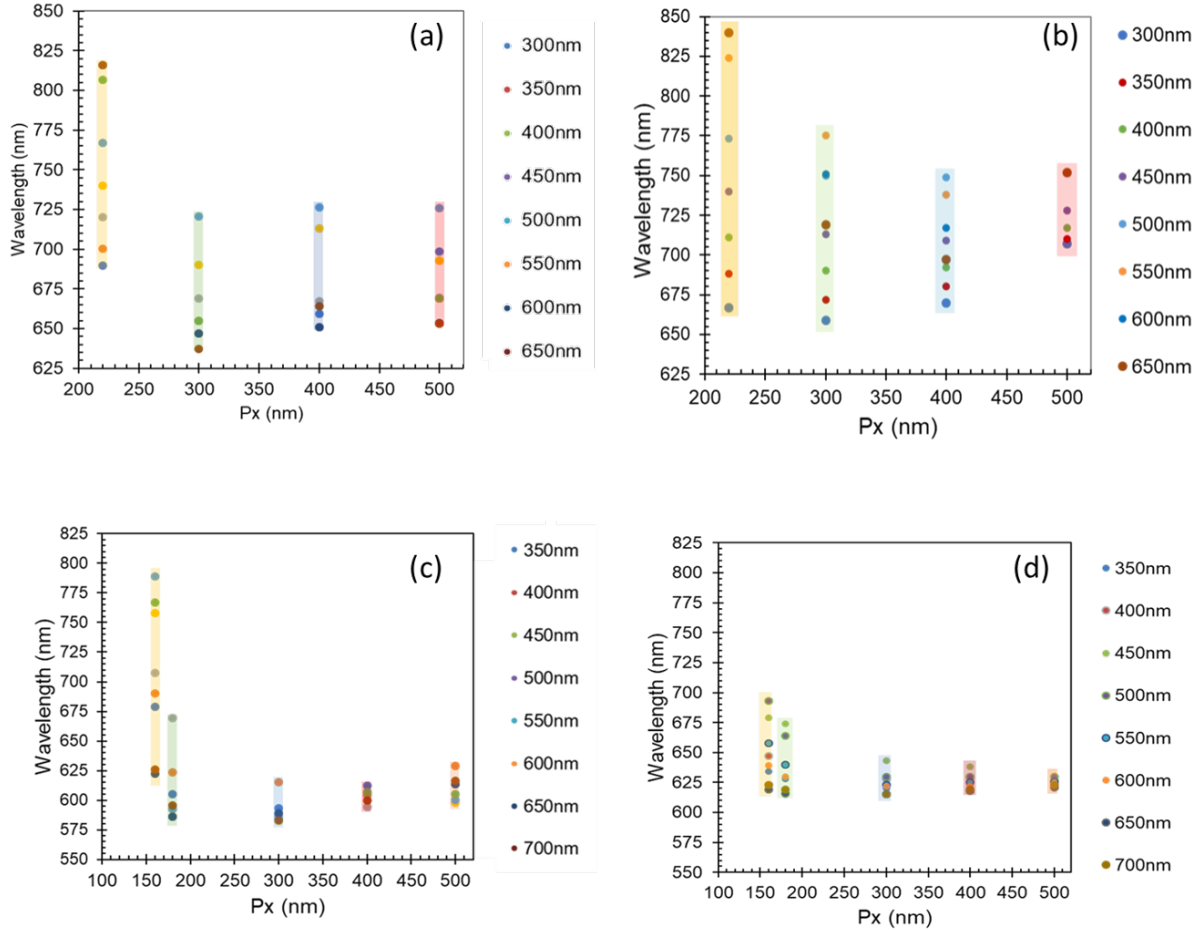


Figure SI 5: Spectral range of the red-shift in the SLR when varying the grating constant P_Y for different P_X values: (a) and (b): experimental and calculated SLR wavelengths for arrays with disks of $D=150$ nm, respectively. (c) and (d): experimental and calculated SLR wavelengths for arrays with disks of $D=100$ nm, respectively. It demonstrates that as P_X increases, the magnitude of the SLR red-shift decreases with variations in P_Y .

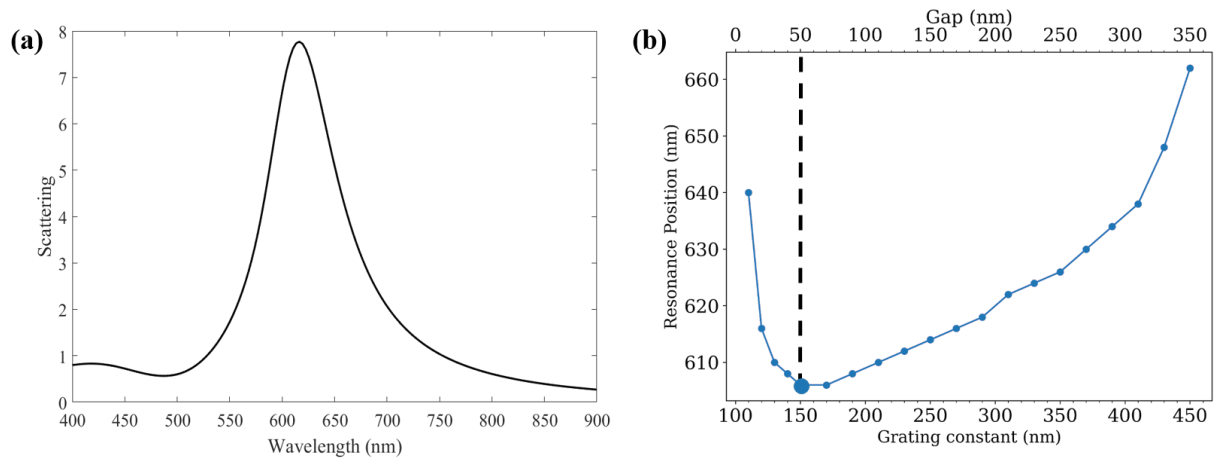


Figure SI 6: (a) Calculated scattering efficiency spectrum of a single gold nanodisk. (b) Resonance wavelengths of square arrays of the same gold nanodisks as a function of the gratings' constant. The nanodisks have a diameter $D=100\text{nm}$ and height $H=50\text{nm}$ and are deposited on a glass substrate and surrounded by air.